Two-Dimensional Acoustic Emission Source Localization on a Laminated Veneer Lumber Plate by Gaussian Process Regression

XIANGDONG HE and XUAN ZHU

ABSTRACT

Acoustic emission (AE) source localization is an important part of monitoring the health of infrastructures. Though straightforward for isotropic materials, where analytical solutions exist, locating sources for anisotropic materials is complicated due to the angle-dependent wave velocity. The problem is even more intractable if heterogeneity involves. This is the case for laminated veneer lumber (LVL), an engineered wood material composed of multiple thin layers of wood, where defects such as knots, voids and discontinuity distributed randomly within the layers, greatly undermining the effectivity of common localization methods for man-made composites. To avoid the problem of heterogeneity, this work employed Gaussian process regression (GPR) to address the 2D AE source localization problem in an LVL plate. With four AE sensors attached at the corner of ROI in the plate, multiple pencil lead break tests were conducted to collect the difference of time of arrival (dTOA) between different sensors. The vector of dTOAs serves used as the input of the Gaussian process regression while the output is the source location. The marginal likelihood was maximized to achieve the optimal model parameters. The input vectors of a different combination of dTOA components were fed into the GPR model, both the predictions on grid points and off-grid points were analyzed. The high accuracy of the mean predictions over all possible combinations of dTOAs indicates such a method can well cope with 2D source localization problems in LVL structures.

INTRODUCTION

Laminated veneer lumber is one of the most widely used engineered wood for building construction. It consists of multiple thin layers of wood stacked with adhesives, resulting in superior features to that of conventional lumber in higher strength, more reliable mechanical properties as well as less likeliness of wrapping, twisting, bowing or shrinking. A typical LVL plate is shown in Figure 1 with three axes as the longitudinal direction (L), the tangential direction (T), and the radial direction (R). Although there are many studies focusing on investigating the acoustic emission behavior of wood, only

Xiangdong He, PhD Student, Email: xiangdong.he@utah.edu. Infrastructure Sensing Experimental Mechanics (ISEM), Department of Civil and Environmental Engineering, The University of Utah, Salt Lake City, 84112, UT, USA.

a limited number of them studying the LVL. Usually, wood is considered as orthotropic material with L, T, R axis. However, this might not be true for LVL due to the existing knots (the brown dots in top view in Figure 1), flaws, or voids in its manufacturing process.

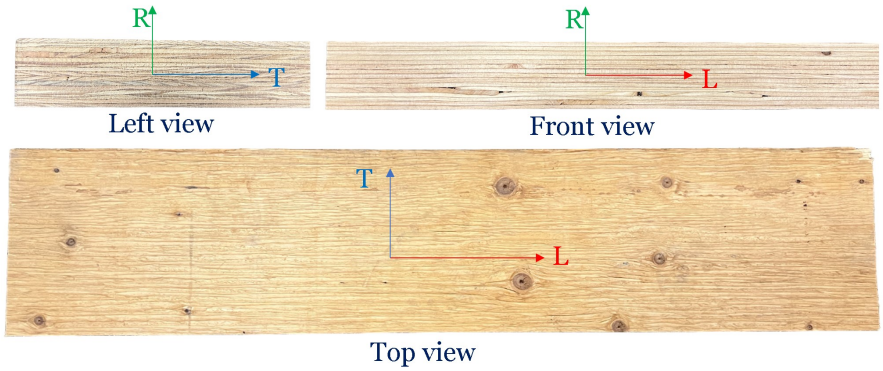

Figure 1. The Laminated Veneer Lumber plate

As a common way for structural health monitoring of infrastructures, acoustic emission testing was considered in this paper to investigate the source location in an LVL plate. In fact, acoustic emission is defined as the release of transient elastic waves generated from a rapid release of strain energy [1]. By attaching piezoelectric sensors (AE sensors) working within a certain frequency range on the monitored structures, waveforms generated by internal micro-cracks can be collected and analyzed.

The source localization is one of the most intriguing features of AE testing. Through analyzing the dTOA between sensor pairs, the source can be located. For isotropic materials, the wave velocity is regarded as a constant. With it known, theoretical solutions can be solved [2]. For man-made composite materials, though their properties are angle-dependent, their textures are uniform, and the wave velocity varies with propagation angle, leading to no theoretical solution. Instead, the source location is typically solved by optimization.

The high degree of heterogeneity of LVL makes the wave travel path unpredictable and invalidates the common methods suitable for man-made composites [3–6]. Fortunately, this issue can be solved by machine learning considering the dTOAs. The unpredictable travel path for LVL is similar to that of the metal plate with holes. The previous research [7] has proven that Gaussian process regression is applicable to the latter problem. This work tried to employ the GPR for wood, the model was trained by maximizing the model evidence instead of the sum of the squared loss used in [7]. Besides, the input dTOA vector of different lengths was analyzed thoroughly. The results suggested that the GPR can handle the source localization problem in LVL plate structure with enough accuracy.

DATA ACQUISITION AND EXPERIMENTS

A Laminated Veneer Lumber (LVL) plate shown in Figure 1 with the dimension of 9 ft by 6.5 inches by 1 inch is used for source localization in this article. A small region of interest (ROI) was drawn on the center of the plate to avoid any boundary

effects. At the same time, a grid with the size of 3.5 inches long and 3.0 inches high was drawn exactly on the ROI, which is shown in Figure 2. Its grid size is 0.25 inches. Four Nano-30 sensors manufactured by Physical Acoustics Corporation were mounted on the four corners of the grid with wax. The four corners marked by brown color were neglected since they are too close to the sensors and the waveforms may not be accurate. Each sensor was then connected to an amplifier followed by the terminal of the Physical Acoustic AE system.

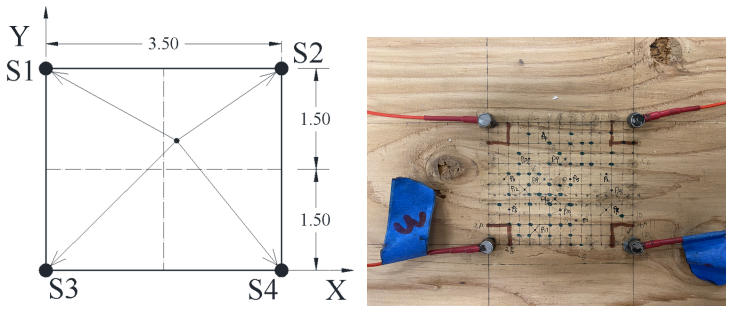

(a) Sensor Location (b) Region of Interest

Figure 2. Layout of the grid (Unit: inch)

The pre-step is constructing a databank where the waveforms generated by the pencil break tests on all the grid points were stored there. However, for source localization, only the first part of the waves is of interest because the P-wave always arrives at the sensors first. The dTOA (difference of time of arrival) of between sensor pairs were extracted. The onset of wave was determined by AIC (Akaike Information Criterion) picker. At least 10 pencil break tests were conducted at each grid point. Instead of taking the mean of all the tests on each grid point, all the reasonable dTOAs were kept to allow for uncertainty during the tests. The grid's origin is set at the bottom left corner of the grid. Given a position vector field:

$$\boldsymbol{r} = (x_i, y_j), (i, j = 1, 2, 3, \ldots, N) \tag{1}$$

The measurements are:

$$\Delta \mathrm{T} = [t_{12}, t_{13}, t_{14}, t_{23}, t_{24}, t_{34}]^{\mathrm{T}} \tag{2}$$

The relation between the position vector and the measurement vector is a one-to-one mapping. This study aims at investigating such mapping through machine learning. The relation between the measured difference of time of arrival between different sensor pairs and the source coordinates can be represented as

$$\boldsymbol{r} = f(\Delta \mathrm{T}) \tag{3}$$

The problem then comes down to learning the mapping from the measured ΔT vector to the source location $\boldsymbol{r}$, which is a regression problem. Since there are six components in the ΔT vectors, it is feasible only to use part of them, where a Bayesian sampling space is constructed. Each scheme corresponds to a model, the total is $6+15+20+15+6+1 = 63$, obtained by the combinations.

2D AE SOURCE LOCALIZATION BY GAUSSIAN PROCESS REGRESSION

Once the data collection job is done, the training databank is available. It contains roughly 2200 measurements, while there are 10 off-grid test points and 10 grid test points where at least 5 tests were repeated in each individual test point location to allow for uncertainties.

In GPR, the training dataset and the test data are combined and assumed to obey the multivariate Gaussian distribution. The joint distribution of the noisy training samples $(\boldsymbol{X}, \mathbf{y})$ together with the prediction of the test data $(\boldsymbol{X}_*, \boldsymbol{f})$ is,

$$\begin{bmatrix} \mathbf{y} \\ \boldsymbol{f}_* \end{bmatrix} \sim N\left(\mathbf{0}, \begin{bmatrix} \boldsymbol{K}(\boldsymbol{X}, \boldsymbol{X}) + {\sigma_n}^2 \boldsymbol{I} & \boldsymbol{K}(\boldsymbol{X}, \boldsymbol{X}_*) \\ \boldsymbol{K}(\boldsymbol{X}_*, \boldsymbol{X}) & \boldsymbol{K}(\boldsymbol{X}_*, \boldsymbol{X}_*) \end{bmatrix}\right) \tag{4}$$

Where the radial basis function is considered and serves as a kernel here to compute the covariance between the random variable $\mathbf{x}_p$ and $\mathbf{x}_q$, which is the two ΔT vectors in this study.

$$\mathrm{k}(\mathbf{x}_p, \mathbf{x}_q) = \alpha \mathrm{exp}\left(-\frac{||\mathbf{x}_p - \mathbf{x}_q||^2}{2\sigma^2}\right) \tag{5}$$

Through matrix derivation, the posterior given the training dataset and the test input also observes the Gaussian distribution [8]

$$\boldsymbol{f}_* | \boldsymbol{X}_*, \boldsymbol{X}, \mathbf{y} \sim N(\bar{\boldsymbol{f}}_*, \boldsymbol{\Sigma}) \tag{6}$$

Where

$$\bar{\boldsymbol{f}}_* = \boldsymbol{K}(\boldsymbol{X}_*, \boldsymbol{X})[\boldsymbol{K}(\boldsymbol{X}, \boldsymbol{X}) + {\sigma_n}^2 \boldsymbol{I}]^{-1} \mathbf{y} \tag{7}$$

$$\boldsymbol{\Sigma} = \boldsymbol{K}(\boldsymbol{X}_*, \boldsymbol{X}_*) - \boldsymbol{K}(\boldsymbol{X}_*, \boldsymbol{X})[\boldsymbol{K}(\boldsymbol{X}, \boldsymbol{X}) + {\sigma_n}^2 \boldsymbol{I}]^{-1} \boldsymbol{K}(\boldsymbol{X}, \boldsymbol{X}_*) \tag{8}$$

The evidence of the training dataset also satisfies the Gaussian distribution

$$\mathbf{y} | \boldsymbol{X} \sim N(\mathbf{0}, \boldsymbol{K}(\boldsymbol{X}, \boldsymbol{X}) + {\sigma_n}^2 \boldsymbol{I}) \tag{9}$$

There are three hyperparameters in GPR, which is α, σ in equation (5), and σ_n in equation (4). The Gaussian process model was trained by maximizing the evidence of all 63 models, corresponding to different number of components for the ΔT vector. The final predictions are the mean predictions over all the possible models with the optimal hyperparameters.

RESULTS AND DISCUSSIONS

The root mean squared error δ_{rmse} was used to measure the prediction performance.

$$\delta_{rmse} = \sqrt{\sum_{i=1}^{N} \frac{1}{N} ||\hat{\boldsymbol{r}}_i - \boldsymbol{r}_i||^2} \tag{10}$$

Once the evidences of all the 63 models were maximized, the training process was completed. The predictions for 10 off-grid test points and 10 grid test points are shown

in Figure 3, respectively. The large and dim symbols show the ground truth, while the thicker one shows the mean predictions, the rest points show the prediction for a single measurement. A same shape shows the predictions for each individual test point.

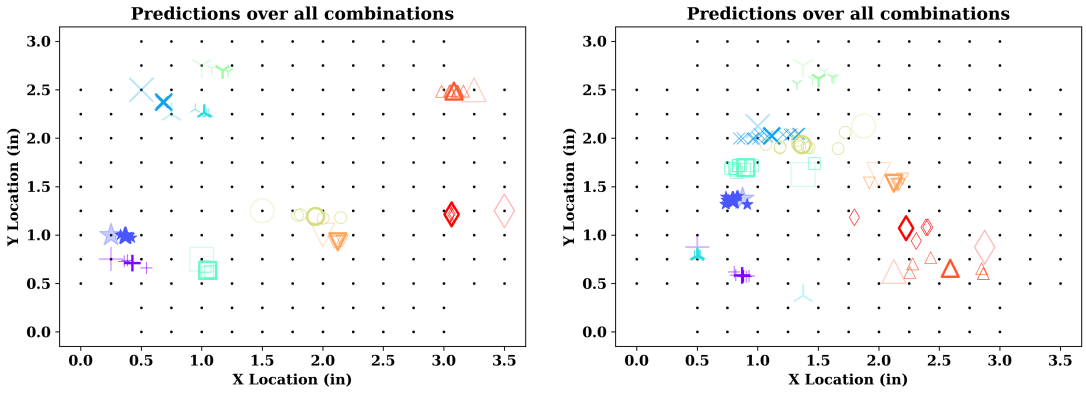

(a) On grid points

(b) On off-grid points

Figure 3. Predictions by GPR over all models

The average rmse of using a different number of components showed different errors. The results for grid test points and off-grid test points are 0.27 inches and 0.52 inches, corresponding to Figure 3 (a) and (b) respectively. Since the training data are exactly on the grid, it is reasonable that the root mean square errors for grid points are smaller than that of the off-grid points. Clearly, the average errors for off-grid points are about two times that of the grid size. This is acceptable since the diameter of the sensor is about 0.4 inches, and the accuracy cannot be smaller than the diameter of the sensor.

CONCLUDING REMARKS

The input ΔT vector of different number of dTOAs was tried, which correspond to different models. The evidences of all the models were maximized to achieve optimal model parameters. As expected, the prediction results on grid points have higher accuracy than those on off-grid points due to that the training data are on the grid nodes. Overall, the predictions are accurate and the GPR can handle the source localization problem on LVL plate structures.

REFERENCES

1. Shull, P. J. 2002. *Nondestructive evaluation : theory, techniques, and applications*, M. Dekker, ISBN 0824788729.
2. Grosse, C. U., M. Ohtsu, D. G. Aggelis, and T. Shiotani. 2021. *Acoustic emission testing: Basics for research–applications in engineering*, Springer Nature.
3. Kundu, T., S. Das, S. A. Martin, and K. V. Jata. 2008. "Locating point of impact in anisotropic fiber reinforced composite plates," *Ultrasonics*, 48:193–201, ISSN 0041624X, doi:10.1016/j.ultras.2007.12.001.

4. Kundu, T., H. Nakatani, and N. Takeda. 2012. “Acoustic source localization in anisotropic plates,” *Ultrasonics*, 52:740–746, ISSN 0041624X, doi:10.1016/j.ultras.2012.01.017.
5. Ciampa, F. and M. Meo. 2010. “A new algorithm for acoustic emission localization and flexural group velocity determination in anisotropic structures,” *Composites Part A: Applied Science and Manufacturing*, 41:1777–1786, ISSN 1359835X, doi:10.1016/j.compositesa.2010.08.013.
6. Ciampa, F., M. Meo, and E. Barbieri. 2012. “Impact localization in composite structures of arbitrary cross section,” *Structural Health Monitoring*, 11:643–655, ISSN 14759217, doi:10.1177/1475921712451951.
7. Hensman, J., R. Mills, S. G. Pierce, K. Worden, and M. Eaton. 2010. “Locating acoustic emission sources in complex structures using Gaussian processes,” *Mechanical Systems and Signal Processing*, 24:211–223, ISSN 08883270, doi:10.1016/j.ymssp.2009.05.018.
8. Rasmussen, C. E. and C. K. I. Williams. 2006. *Gaussian processes for machine learning*, MIT Press, ISBN 026218253X.